Characterization of ion implantation in Si using infrared spectroscopy with a Lock-in Common-Mode-Rejection Demodulation

F. Rábago[1,2], A. Mandelis[2] and A. Salnick[3]

[1]Instituto de Física, Universidad Autónoma de San Luis Potosí
S.L.P., México, rabago@dec1.ifisica.uaslp.mx
[2]Photothermal and Optoelectronic Diagnostics Laboratories,
University of Toronto, Toronto, Canada
[3]Therma Wave Inc., Fremont, CA, USA

ABSTRACT

B^+, P^+, and As^+ ion-implanted Si wafers in the implantation dose range $1x10^{11}$ – $1x10^{13}$ ions/cm^2 were characterized using Photothermal Radiometry (PTR). A comparison between the conventional frequency scan and a new technique called Common-Mode-Rejection Demodulation (CMRD) was done. It was found that the CMRD technique can significantly enhance the resolution of PTR response curves from P^+ ion implanted wafers in cases were conventional square wave frequency scans were totally or partially unable to resolve the dose. The dose resolution improvements afforded by the CMRD technique may be important toward better control of the ion implantation process in electronic devices, in a dose range which has traditionally been difficult to monitor optically owing to the effects introduced by the early stages of the amorphization process in the implanted layer.

Keywords: Semiconductors, ion implantation, photothermal radiometry.

1 INTRODUCTION

The present work has the objective to compare between a conventional frequency-domain PTR [1] and a CMRD PTR.

The CMRD technique is a new demodulation method that was tested after a theoretical study [2] in Zr-2.5Nb samples [3]. It takes advantage of the real-time differential action realized by the lock-in amplifier weighing function over the two half periods of the modulated signal. The particular repetitive waveform is shown in Fig. 1. In a given period T the sample is excited by two square-wave pulses separated by a time interval _ having the same intensity I_0 and durations $\__1$ and $\__2$. This particular repetitive waveform is shown in Fig. 1. It is possible to balance the in-phase and quadrature components of the lock-in amplifier response by choosing the appropriates values of $\__1$, $\__2$ and _. This results in enhanced signal dynamic range due to the suppression of the baseline and a substantial improvement in the signal to noise ratio.

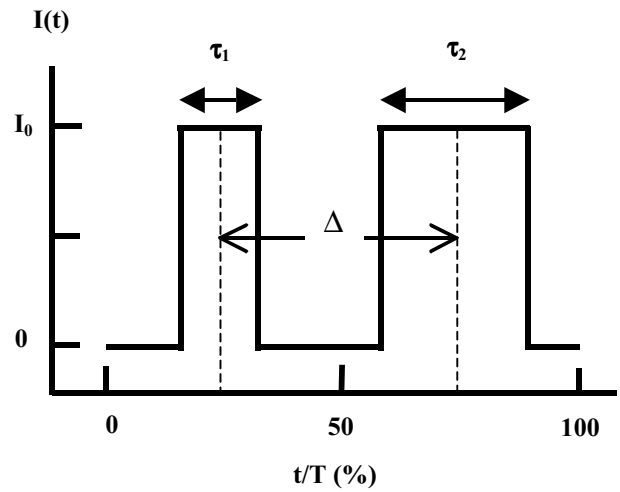

Fig. 1: Optical excitation waveform.

2 EXPERIMENTAL, RESULTS AND DISCUSSION

We report in this work a study made in four sets of five polished 4" wafers. They were implanted with B^+, P^+, and As^+ ions and one of the As^+ set has a oxide. In Table I we show the ion implantation parameters. First, we performed the standard PTR measurements [4]. Furthermore, we change the experimental set-up to do CMRD scans for that we replaced the square-waveform generator connected to the acousto-optic modulator by a programmable waveform synthesizer (Stanford Research System Model DG535). The Ar-ion laser beam (515 nm) was focused to a spot size of ~ 50 _m and an average power of 50 mW. Transients in 2600s duration time scans of the PTR signal at a fixed frequency (4KHz) were performed just before PTR experiments for each sample. The laser was focused in the approximately center point of each wafer and they were tested in the same point for all the experiments. No changes in the reflectivity surface were found for the entire wafer set.

Ion-implant species	Oxide	Dose
As	100 Å	$1x10^{11}$
As	100 Å	$4x10^{11}$
As	100 Å	$1x10^{12}$
As	100 Å	$4x10^{12}$
As	100 Å	$1x10^{13}$
As	Native	$1x10^{11}$
As	“	$4x10^{11}$
As	“	$1x10^{12}$
As	“	$4x10^{12}$
As	“	$1x10^{13}$
P	“	$1x10^{11}$
P	“	$4x10^{11}$
P	“	$1x10^{12}$
P	“	$4x10^{12}$
P	“	$1x10^{13}$
B	“	$1x10^{11}$
B	“	$4x10^{11}$
B	“	$1x10^{12}$
B	“	$4x10^{12}$
B	“	$1x10^{13}$

Table I: Ion implantation parameters.

2.1 PTR frequency and time scans

In the Fig. 2 is shown the typical set of frequency response curves for the set of five wafers implanted with P^+ ions. The amplitude figure is better resolved than the phase. For all wafers implantation groups the same shape curves were found.

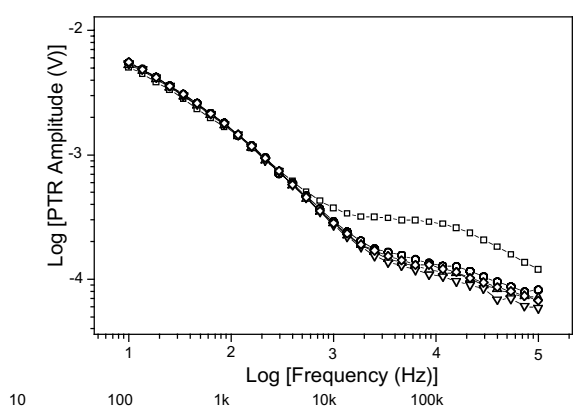

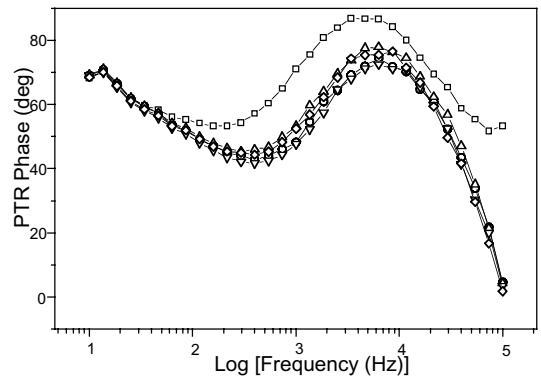

Fig. 2: a) PTR amplitude and b) PTR phase frequency scans of P^+ ion-implanted Si wafers at 100 keV. Doses (ions/cm^2): (_) 1×10^{11}; (O) 4×10^{11}; (Δ) 1×10^{12}; (∇) 4×10^{12}; (◊) 1×10^{13}

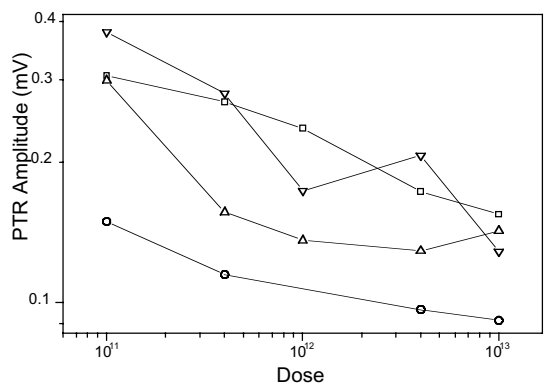

Fig. 3: PTR frequency-scan amplitude dependencies on implantation dose at 4 kHz. (∇): B^+; (Δ): P^+; (O): As^+ (unoxidized); (_): As^+ (with 100- Å thick oxide layer).

In the fig. 3 is presented a summary of the experimental results for all the sets of wafers. This figure was made taking the amplitude at 4 KHz. Here we see a decreasing order of PTR amplitudes with increasing dose and with increasing ionic mass (B, P and As), with the exception of the anomalous $4x10^{12}$ cm^{-2} B^+ and $1x10^{13}$ cm^{-2}. P^+ ion implants.

In the fig. 4 it is shown time scans at 4 KHz PTR amplitudes and phases of the four P^+ implanted wafers ($4x10^{11}$ -$1x10^{13}$ cm^{-2}). We appreciate a nearly overlapped in the amplitudes signals. The relative levels of these curves are consistent with the amplitudes shown in Fig. 2a at the same frequency. Conventional PTR amplitude time scans for the B implanted wafers are shown in Fig. 5. One more time, the relative levels of these curves are consistent with the order of frequency scan amplitudes (shown in Fig. 3).

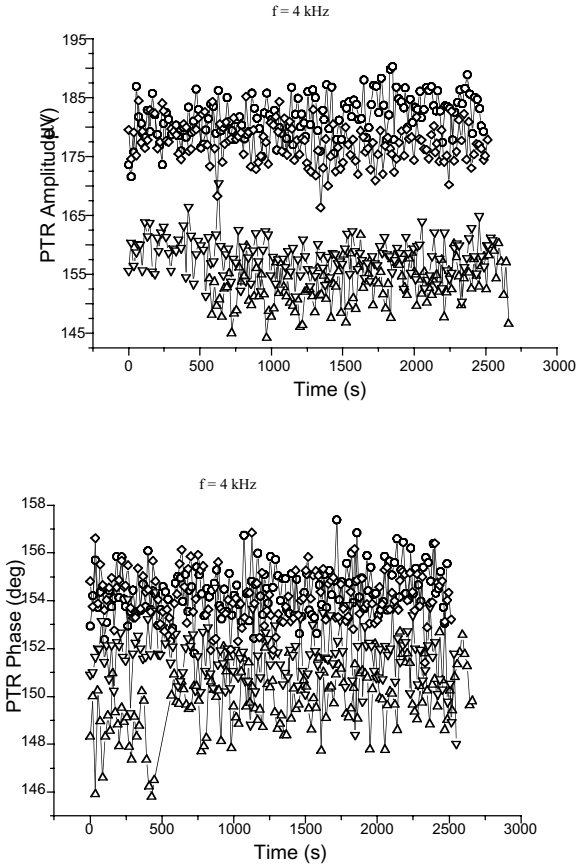

Fig. 4: PTR amplitude a) and phase b) as a function of time for four P silicon wafers at 4 KHz. Doses (ions/cm^2): (O) 4×10^{11}; (Δ) 1×10^{12}; (∇) 4×10^{12}; (◊) 1×10^{13}

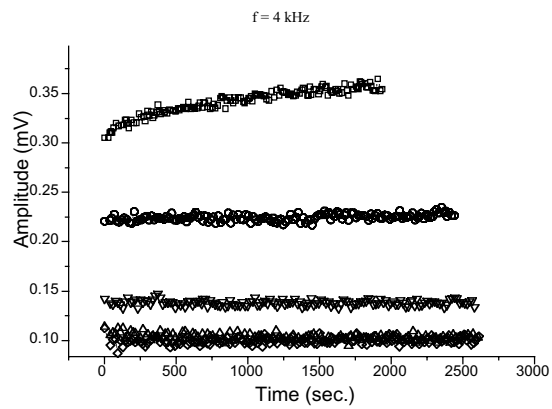

Fig 5: PTR amplitude of the B implanted Si wafers as a function of time. Doses (ions/cm^2): (_) 1×10^{11}; (O) 4×10^{11}; (Δ) 1×10^{12}; (∇) 4×10^{12}; (◊) 1×10^{13}

2.2 PTR CMRD scans

The CMRD method was applied to all the wafers. The measurements were achieved at 4 kHz and _1= 5ms , _2 = 25ms. In the figure 6 is shown only the amplitude and quadrature signals for the four CMRD signal outputs (amplitude, phase, IP, and Q) for the P^+ wafers using __=5% pulse separation increments. The amplitude and quadrature signals were optimal in terms of dose resolution. CMRD measurements (Fig. 6) gave a better resolution than either frequency scan (Fig. 2) or time scan (Fig. 4) due to noise suppression. Only the overlap between the $1x10^{12}$ and $4x10^{12}$ cm^{-2} doses remains essentially unresolved. It is expected that the size of the increments __ may control the dose resolution of the technique, therefore we made, for P set of wafers, CMRD scans with __=1% in the "flat" region between 40 – 49%. In Fig. 7 is shown the corresponding curves. The narrower range __=1% increment scan is

capable to a superior and complete resolution of the $1x10^{12}$ and $4x10^{12}$ cm^{-2} doses curves.

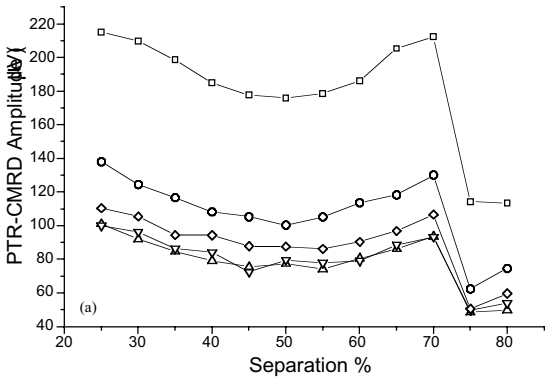

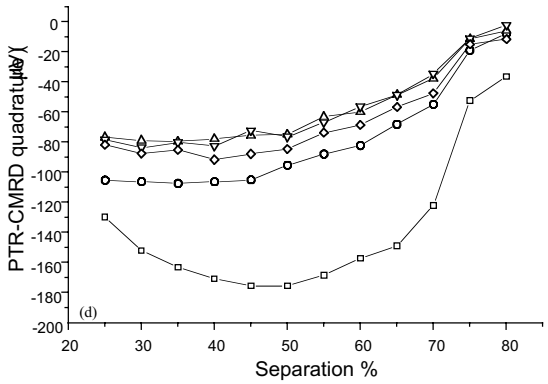

Fig. 6: a) Amplitude, and d) quadrature of the PTR-CMRD signal output of P^+ implanted Si wafers. Doses (ions/cm^2): (_) 1×10^{11}; (O) 4×10^{11}; (Δ) 1×10^{12}; (∇) 4×10^{12}; (◊) 1×10^{13}

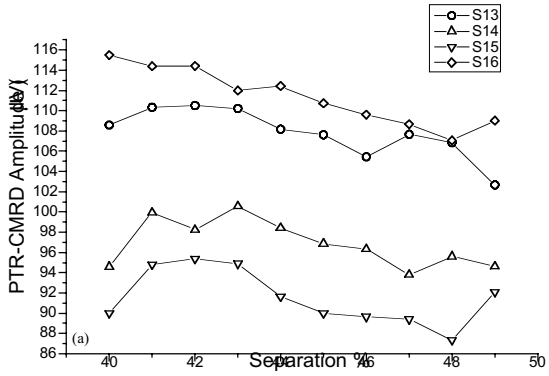

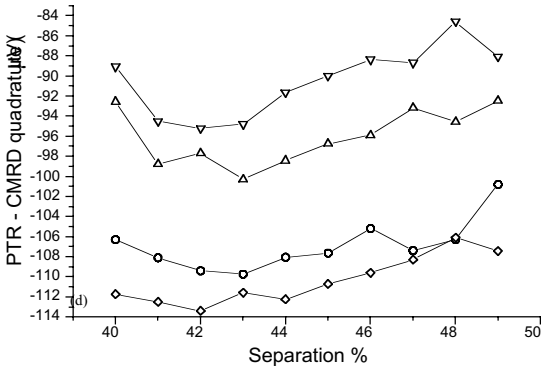

Fig. 7: High resolution PTR-CMRD amplitude a) and quadrature d) signals from the P^+ implanted wafers v.s. center to center pulse separation _(%). Doses (ions/cm^2): (O) 4×10^{11}; (Δ) 1×10^{12}; (∇) 4×10^{12}; (◊) 1×10^{13}. Pulse separation increment __=1%.

3 CONCLUSIONS

A new PTR-CMRD technique was introduced to measure Si wafers implanted with B^+, P^+, and As^+ (with and without a surface oxide) in a very narrow implantation dose range $1x10^{11}$-$1x10^{13}$ ions/cm^2. The conventional photothermal probes have some difficulties to distinguish such as narrow ion implantation dose range. We found that CMRD can significantly enhance the dose resolution of the PTR response curves from P^+. With the conventional square wave frequency scans were totally or partially unable to resolve the doses. CMRD enhancement over the conventional frequency scan amplitude occurs in $1x10^{12}$-$1x10^{13}$ ions/cm^2 where conventional frequency scans are completely overlapped. These CMRD advantages is due to the fact that the waveform (Fig. 1) effectively suppresses the signal background and noise levels. The most important parameter of the CMRD method is the pulse separation increment __, because it controls the dose resolution capabilities through suppression of the instrumental signal and noise baseline levels of the technique.

The CMRD technique can be important for application in semiconductor industry to monitor the ion implantation step.

4 ACKNOWLEDGEMENTS

F. Rábago wish to thank Conacyt-México for the sabbatical scholarship and Universidad Autónoma de San Luis Potosí.

REFERENCES

[1] M. E. Rodríguez, A. Mandelis, G. Pan, L. Nicolaides, J. A. García and Y. Riopel, J. Electrochem. Soc., **147**, 687, 2000.

[2] A. Mandelis, S. Paoloni and L. Nicolaides, Rev. Sci. Instrum., **71**, 2440, 2000.

[3] S. Paoloni, L. Nicolaides and A. Mandelis, Rev. Sci. Instrum., **71**, 2445, 2000.

[4] A. Mandelis and Y. Riopel, J. Vacc. Sci. Technol., **A 18**, 705, 2000.